IEEE Access
Multidisciplinary | Rapid Review | Open Access Journal

Received 20 June 2023, accepted 23 July 2023, date of publication 26 July 2023, date of current version 8 August 2023.

Digital Object Identifier 10.1109/ACCESS.2023.3299170

RESEARCH ARTICLE

Miniaturized Inline Bandpass Filters Based on Triple-Mode Integrated Coaxial-Waveguide Resonators

MUHAMMAD YAMEEN SANDHU[1], (Senior Member, IEEE), SHARJEEL AFRIDI[1], (Senior Member, IEEE), ADAM LAMECKI[2], (Senior Member, IEEE), ROBERTO GÓMEZ-GARCÍA[3], (Fellow, IEEE), AND MICHAL MROZOWSKI[2], (Fellow, IEEE)

[1]Department of Electrical Engineering, Sukkur IBA University, Sukkur 65200, Pakistan
[2]Faculty of Electronics, Telecommunications, and Informatics, Gdańsk University of Technology, 80-233 Gdańsk, Poland
[3]Department of Signal Theory and Communications, Polytechnic School, University of Alcalá, 28871 Alcalá de Henares, Spain

Corresponding author: Muhammad Yameen Sandhu (m.y.sandhu@ieee.org)

This work was supported in part by the Polish National Science Centre under Grant UMO-2019/33/B/ST7/00889, and in part by the Gdańk University of Technology (ARGENTUM Grant under the Excellence Initiative–Research University) under Grant DEC–54/2020/IDUB/I.3.3.

ABSTRACT This work presents a design technique to implement miniaturized cross-coupled bandpass filters in inline physical configurations based on triple-mode resonators. Triple-mode resonances are obtained by using integrated coaxial-waveguide cavity resonators. They consist of two coaxial conducting posts placed in the sidewalls of a rectangular waveguide cavity. In the proposed triplet, a transmission zero (TZ) can be positioned at any of the two sides of the passband by simply locating the coaxial posts either on the same wall or on opposite walls of the rectangular waveguide cavity. Coaxial-to-waveguide mode coupling is implemented by means of coupling screws, which adds flexibility in terms of tuning easiness. Three 9.9-GHz proof-of-concept prototypes corresponding to third- and sixth-order integrated coaxial-waveguide bandpass filters are designed at the electromagnetic-simulation level. Furthermore, the triplet with a TZ below the passband is manufactured and characterized to experimentally validate the engineered 3-D RF filter principle and its underlying design theory.

INDEX TERMS 3-D filter, bandpass filter, coaxial filter, inline filter, microwave filter, transmission zero (TZ), waveguide filter.

I. INTRODUCTION

Waveguide and coaxial-cavity bandpass filtering devices are commonly used in transceiver RF front-ends of modern communication systems to efficiently acquire the desired signal band and suppress out-of-band interference and noise [1], [2], [3], [4]. The current tightly-spaced spectrum-allocation planning requires highly-selective bandpass filters with sharp-rejection responses. Besides, in order to accommodate the ever-increasing number of RF chains to support emerging multi-input-multi-output (MIMO) applications, the transceiver architecture is evolving towards miniaturized implementations requiring highly-compact RF components. Filter selectivity can be increased by augmenting its order through the incorporation of more resonators but at the expense of increased size/volume and higher in-band insertion loss, which may be unacceptable for lightweight and high-performance RF communication transceivers. Alternatively, transmission zeros (TZs) are commonly exploited to increase the selectivity in RF bandpass filters. They can be

The associate editor coordinating the review of this manuscript and approving it for publication was Derek Abbott.

realized by creating cross couplings between nonadjacent resonators in the form of triplets [5], [6], [7] or quadruplets [8], [9], [10], [11] to produce destructive RF signal interferences, as well as through their combination in cascaded or folded forms. In the past decade, significant effort has been carried out to develop filters with TZs in inline configurations, both in waveguide and coaxial-resonator technologies. Thus, several design approaches of inline waveguide bandpass filters with TZs using frequency-dependent couplings have been reported as in [9], [12], [13], and [14]. For inline coaxial combline filters, cross couplings can be produced by rotating the inner cylinders to shape pseudo-elliptic-type filtering responses [15], [16], [17]. In [18] and [19], strongly-coupled coaxial-resonator pairs are used to implement inline bandpass filters with TZs. In [20], several inline schemes for coaxial combline filters with TZs are presented.

The design process of a volume-efficient dual-resonance integrated coaxial-waveguide-resonator bandpass filter is reported in [21]. The suggested dual-resonance cavity consists of a rectangular metallic enclosure with a partial-height post placed horizontally in-parallel to its broadwall. Its geometry was optimized so that the fundamental resonance of the waveguide mode coincides with the second resonance of the post. Coaxial-to-waveguide mode coupling was implemented by connecting the broadwall of the metallic enclosure to the loading post by using an auxiliary probe. This work was further extended in [22], where the post was replaced by a re-entrant resonator and the inter-resonator coupling mechanism was modified to allow post-fabrication tuning capability.

To further miniaturize the volume/size of the overall 3-D bandpass filter, an alternative way is to excite triple modes in a resonator. Several design approaches for triple-mode-resonator-based RF filters have been reported in the literature; for example, among them, those exploiting dielectric-loaded resonators [23], [24], corner-cut cavities [25], conductor-loaded triple-mode cavitties [26], circular triple-mode cavities [27], stubbed waveguide cavities [28], angled-slot-excited cavities [29], or metallic-post-loaded source-load coupled triple-mode resonant cavities [30], [31]. However, these multimode filters usually suffer from poor spurious performance and complicated cross-coupling realizations, also requiring complex tuning mechanisms.

In this work, the design of a class of triple-resonance integrated coaxial-waveguide-resonator triplet bandpass filters is presented. As shown in Section II, the synthesized triplet consists of a simple rectangular waveguide section with two conducting metallic posts placed at the waveguide sidewalls. The posts are located at the same plane to create a TZ above the passband and at opposite planes to flip the TZ below the passband. Using this triple-mode coaxial-waveguide resonator approach, two triplet bandpass filters with a TZ below and above the passband and a sixth-order filter with TZs at both passband sides are designed at the electromagnetic-simulation level in Sections III, IV, and V, respectively. Furthermore, for experimental-validation purposes, a 9.9-GHz prototype of a triplet filter with a TZ below the passband is developed and measured in Section VI.

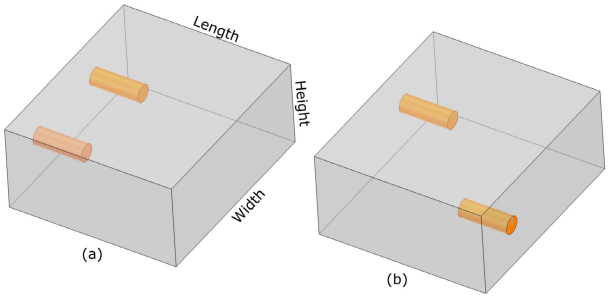

FIGURE 1. Geometry of the proposed integrated coaxial-waveguide resonator. (a) Both posts located at the same side wall. (b) Posts located at opposite side walls.

II. TRIPLE-MODE COAXIAL-WAVEGUIDE RESONATOR

A half-wavelength rectangular-waveguide section with two conducting posts placed at its sidewalls—i.e., narrow wall either at the same plane (SP) or at opposite planes (OP) as illustrated in Fig. 1(a) and (b), respectively—produces three resonances allocated in the close proximity. Each resonance frequency can be tuned independently to shape a bandpass frequency response. One of the resonances is associated with the fundamental TE_{10} waveguide mode, whereas the other two are produced by the coaxial TEM resonators formed by the partial-height conducting posts. The conducting-post loading of the half-wavelength-long resonator allows further reducing the size of the cavity. For both the SP and OP arrangements of the posts, the posts are symmetrically placed and the resonance frequencies associated with these posts can easily be controlled by the height of the posts. To determine the quality factor (Q) associated to the resonance of each post and the waveguide mode, the structure was simulated in the eigensolver of HFSS with finite-conductive boundary conditions. Aluminium boundary was assigned to both posts and the cavity. The Qs corresponding to the post resonances are found to be 2670 and 2649, whereas the Q associated to the waveguide-mode resonance is 5662. The E and H-field patterns of the coaxial-mode resonances corresponding to the partial-height conducting posts arranged in SP or OP arrangement, computed through the eigensolver of HFSS software, are plotted in Figs. 2 and 3, respectively. The H-field pattern associated to the waveguide-mode resonance for both the SP and OP post arrangements is shown in Fig. 4. From Figs. 2-4, it is observed that the E and H-fields of the waveguide and coaxial-mode resonances are perpendicular to each other. To design a bandpass filter, all three modes need to be coupled with one another. For both the SP and OP configurations, the coupling coefficient between post resonances can be controlled by adjusting the spacing between the posts. Graphs of the coupling coefficients as a function of the separation between the posts are represented in Fig. 5.

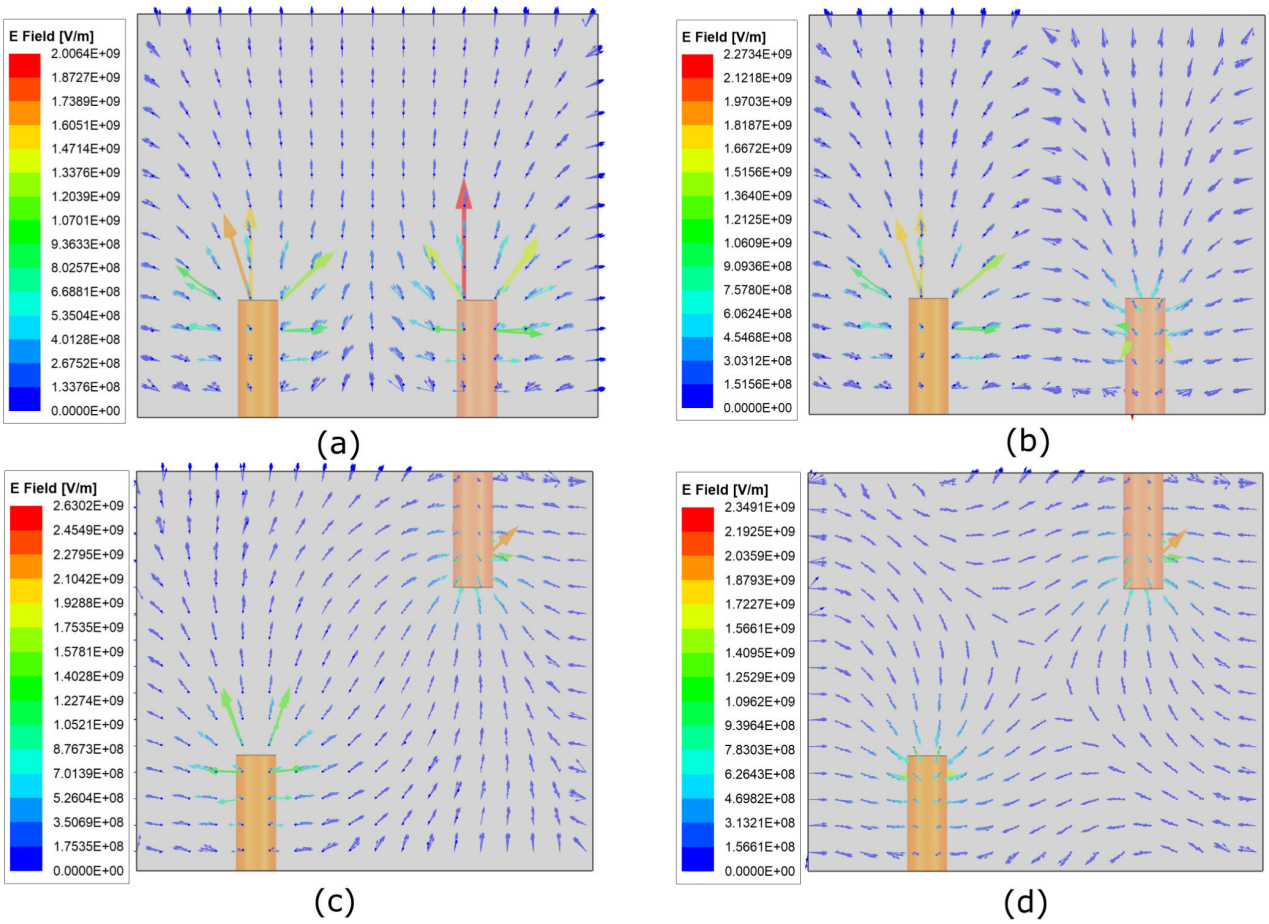

FIGURE 2. *E*-field distributions for coaxial modes. (a) Even and (b) odd mode for same-side posts. (c) Even and (d) odd mode for opposite-side posts.

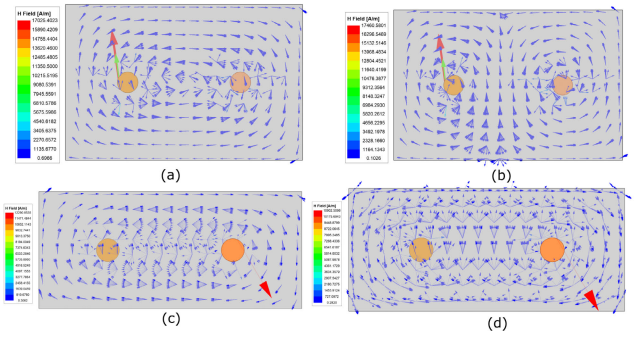

FIGURE 3. *H*-field distributions for coaxial modes. (a) Even and (b) odd mode for same-side posts. (c) Even and (d) odd mode for opposite-side posts.

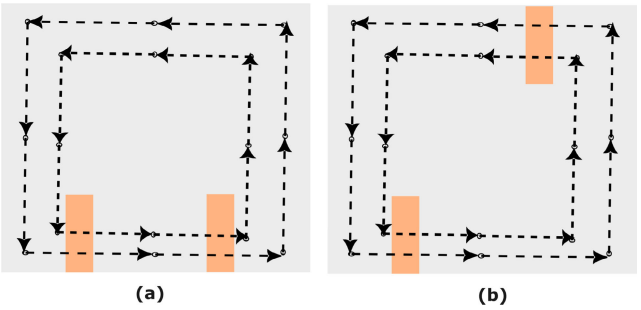

FIGURE 4. *H*-field distributions for the waveguide mode. (a) Same-side posts. (b) Opposite-side posts.

Based on different variants of the devised triple-mode integrated coaxial-waveguide resonator concept, several design examples of RF bandpass filters are subsequently presented.

III. DESIGN EXAMPLE I: SAME-SIGN TRIPLET

As the first example, a third-order bandpass filter with center frequency of 9.95 GHz, 300-MHz bandwidth—i.e., equal to 3% in relative terms—, 20-dB minimum in-band input-power-matching level, and a TZ located in the upper stopband at 10.2 GHz is designed. To design the filter as per given specifications and topology, the coupling matrix is synthesized using [32]. The first step in the filter design process is to generate the rational polynomials that represent the desired transmission and reflection parameters, namely S_{21} and S_{11}, respectively. These polynomials are designed to meet the prefixed attenuation mask—i.e., out-of-band rejection

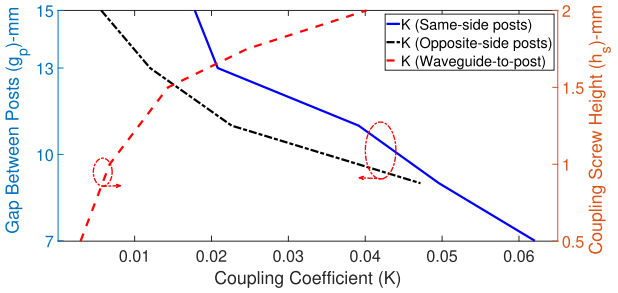

FIGURE 5. Normalized coupling coefficient—i.e., $m_{ij} * BW/f_0$ where f_0 and BW are the center frequency and the bandwidth, respectively—between same-side and opposite-side posts as a function of the distance between the posts and post-to-waveguide mode coupling as a function of the coupling-screw length.

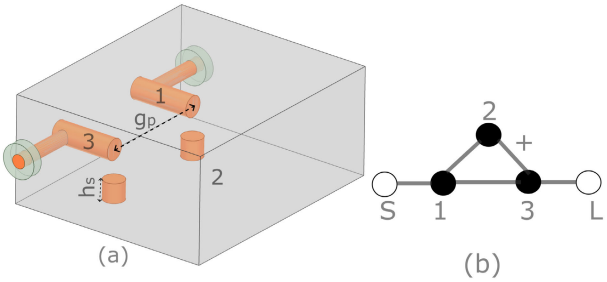

FIGURE 6. Proposed SP triplet filter. (a) Coaxial-in/coaxial-out scheme: upper-side TZ triplet with both posts at the same plane. (b) Coupling-routing diagram (black circles: resonating nodes; white circles: source (S) and load (L); continuous lines: couplings).

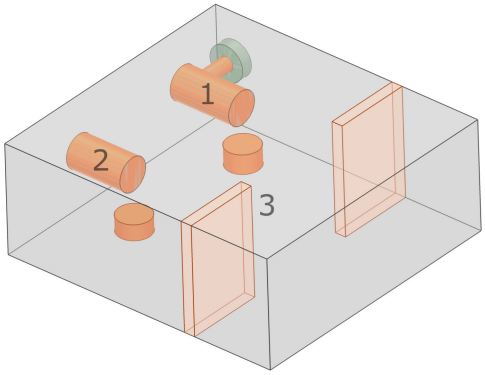

FIGURE 7. Coaxial-in/waveguide-out scheme: upper-side TZ triplet with both posts at the same plane.

and in-band requirements—of the intended application. Their mathematical expressions are as follows (ω is the angular frequency):

$$S_{11}(\omega) = \frac{F(\omega)}{\epsilon_R E(\omega)} \tag{1}$$

$$S_{21}(\omega) = \frac{P(\omega)}{\epsilon E(\omega)} \tag{2}$$

where

$$\epsilon = (1/\sqrt{1 - 10^{-\mathrm{RL(dB)}/10}}).\frac{P(\omega)}{F(\omega)} \tag{3}$$

with $\epsilon_R = 1$ or $\epsilon_R = \epsilon/\sqrt{\epsilon^2 - 1}$ if the function is fully canonical, and RL(dB) is the prescribed equiripple return-loss level of the Chebyshev-type function in decibels. Once these polynomials are obtained, the next phase involves synthesizing the associated coupling matrix by constructing the two-port short-circuit admittance-parameter matrix $[Y_N]$ from the coefficients of the rational polynomials of the $S_{21}(\omega)$ and $S_{11}(\omega)$ parameters. Specifically, for this design example, the evaluated coupling-matrix entries are $m_{11} = m_{33} = 0.1645, m_{22} = -0.6656, m_{S1} = m_{3L} = 1.0846, m_{12} = m_{23} = 0.8386$, and $m_{13} = 0.7119$.

The filter consists of a rectangular waveguide cavity with two metallic posts (1&3) embedded into it. Specifically, both posts are placed at the same waveguide sidewall to keep all the mainline and cross couplings of the same sign. The filter geometry and coupling-routing diagram with all positive inter-resonator couplings are shown in Fig. 6(a) and hyperref[fig:triplet1](b), respectively. The waveguide box along with the metallic posts is simulated in the eigensolver of HFSS to compute the required resonances and their associated Qs. The external couplings are realized through direct tapping of the metallic coaxial posts, whereas the inter-mode couplings are implemented through easily-adjustable coupling screws placed against the open ends of the posts—i.e., at the waveguide broadwall. The depth h_s of the screw inside the cavity is directly proportional to the realized coupling coefficient. A parametric plot of the coupling coefficient as a function of the inter-post separation to realize the coupling between the posts is presented in Fig. 5. It is evident that stronger coupling occurs as the posts are more-closely spaced. In the same figure, a plot of the coupling coefficient for the post-to-waveguide mode coupling as a function of the coupling-screw length is presented. As an expected result, stronger coupling levels occur for deeper coupling screws.

A fine numerical tuning of the synthesized filter design is finally performed using the zero-pole optimization technique of the commercial FEM-based microwave EDA software InventSim [33], [34]. The 3-D layout of the final optimized third-order bandpass filter is shown in Fig. 6(a) and its electromagnetically-(EM)-simulated scattering parameters are depicted in Fig. 8. The results in Fig. 8 fairly verify the proposed filter design concept, proving that a waveguide resonator loaded with two metallic coaxial posts can be employed to implement a miniaturized inline waveguide bandpass triplet filter with a TZ located above its passband.

In the above example, the operational principle of one variant of the proposed integrated coaxial-waveguide triplet filter—Fig. 6(a)—is demonstrated,in which the external couplings were realized through direct tapping of the coaxial posts. In that design, resonators 1 and 3 in Fig. 6(b) correspond to the coaxial posts, whereas the waveguide resonance constitutes resonator 2. For the design of higher-order filters, it is more appropriate to exploit it as a building block. Another realization of the proposed triplet filter concept is shown in Fig. 7. In this case, the input coupling is realized

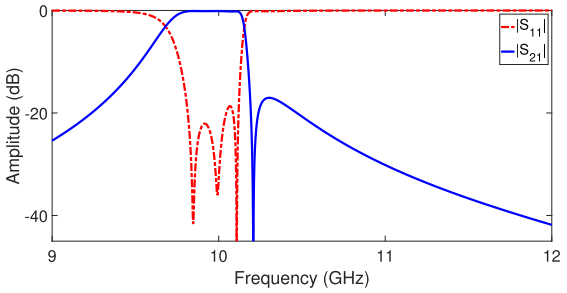

FIGURE 8. EM-simulated power transmission ($|S_{21}|$) and reflection ($|S_{11}|$) responses of the triplet filter examples corresponding to the 3-D layouts shown in Figs. 6(a) and 7.

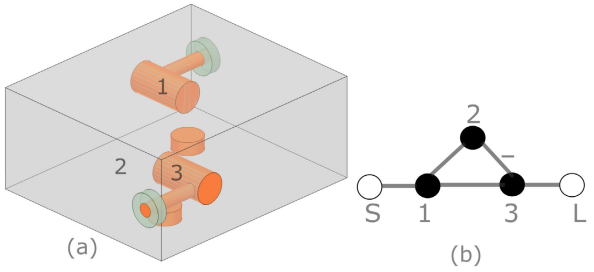

FIGURE 9. Proposed OP triplet filter. (a) Coaxial-in/coaxial-out scheme: Lower-side TZ triplet with both posts placed at opposite planes. (b) Coupling-routing diagram (black circles: resonating nodes; white circles: source (S) and load (L); continuous lines: couplings).

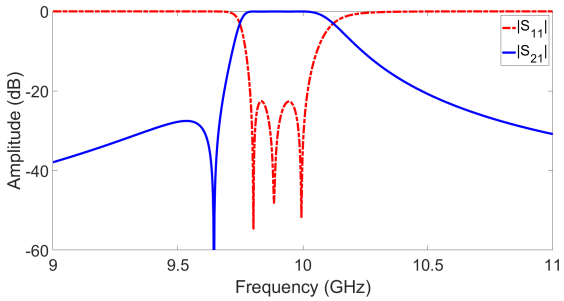

FIGURE 10. EM-simulated power transmission ($|S_{21}|$) and reflection ($|S_{11}|$) responses of the triplet filter example corresponding to the 3-D layout shown in Fig. 9(a).

through direct tapping of one of the coaxial posts (1)—the other post (2) remains untapped—, whereas the output coupling can be realized through an inductive window to an additional output waveguide section. The coupling between resonators 1 and 2—which are now the tapped and untapped posts, respectively—is controlled through the spacing between both posts. On the other hand, the direct coupling between resonators 2 (untapped post) and 3 (waveguide-mode resonance)—and the cross coupling between resonators 1 and 3 are controlled through the coupling screws placed at the waveguide broadwall. It should be noted that in the previous case, both coaxial posts were symmetric because resonators 1 and 3 in the computed coupling matrix have the same resonance frequency. For the asymmetric case, the two posts and the two coupling screws would have different lengths to properly implement resonators 1 and 2 and the corresponding inter-resonator couplings 1–3 and 2–3. The final dimensions of both designed filters in Figs. 6(a) and 7 producing the EM-simulated scattering parameters plotted in Fig. 8 are provided in Table 1.

IV. DESIGN EXAMPLE II: OPPOSITE-SIGN TRIPLET

In Section III, the design of a triplet filter with a TZ located above the passband has been illustrated. However, it is possible to flexibly flip the TZ from above to below the passband by simply relocating one of the posts at the opposite side wall of the waveguide cavity, as shown in Fig. 9(a). This is due to the fact that the H-field in a waveguide resonator forms horizontal circles in the cavity parallel to its broadwall, travelling in opposite direction along the opposite sidewalls of the cavity. Therefore, when both posts are placed at the same plane, they interact with the waveguide mode H-field of same sign. For the case of posts placed at the opposite sidewalls, each post interacts with the waveguide mode H-field of reversed polarity. A plot of the H-field associated with the waveguide mode of the proposed integrated coaxial-waveguide triplets with the posts arranged in SP and OP arrangements is shown in Fig. 4. It is evident that for the SP case, both posts interact with the same-polarity H-field of the waveguide mode whereas for the OP case, each post interacts with opposite-polarity H-field of the waveguide mode. This reverses the sign of the couplings between the input post (1) and the waveguide (2) mode and from the waveguide (2) mode to the output post (3). As further validation, the design of a third-order bandpass filter with 9.9-GHz center frequency, 200-MHz bandwidth—i.e., relative bandwidth of 2%—, 20-dB minimum in-band return-loss level, and a TZ located at the lower stopband is demonstrated. The evaluated coupling-matrix entries for the given specifications and topology are $m_{11} = m_{33} = -0.108$, $m_{22} = 0.4222$, $m_{S1} = m_{3L} = 1.0827$, $m_{12} = 0.9598$, $m_{23} = -0.9598$, and $m_{13} = 0.4377$.

The synthesis process is exactly the same as described in Section III with the only difference being that the posts are placed this time at the opposite sidewalls of the waveguide—rather than at the same sidewall—so that to produce the TZ below the filter passband. As revealed by the results in Fig. 5, the inter-post coupling coefficient is smaller for opposite-side posts when compared to same-side posts for a similar separation between posts. The physical 3-D layout of the EM-simulated third-order waveguide bandpass filter geometry along with its coupling topology with negative 2–3 coupling sign are shown in Fig. 9(a) and (b), respectively. The EM-simulated scattering parameters corresponding to the filter example in Fig. 9(a) with dimensions listed in Table 1 are represented in Fig 10. The obtained results—along with those of Section III—corroborate that by using integrated coaxial-waveguide resonators, inline quasi-elliptic-type bandpass filters with a TZ located at either side of the passband can be designed by placing the posts either at the same or opposite sidewalls of the waveguide.

TABLE 1. Final dimensions of the designed filters.

Parameters (mm)	SST filter	SST filter (waveguide out)	OST filter (fabricated)	Sixth-order filter
Cavity width and height	22.91×10.16	24.6×10	23×10	21.27×9.79
Cavity lengths	19.51	18	19.6	21.66, 21.73
Tapped posts heights	5.87, 5.87	5.8	5.65, 5.65	5.72, 5.69
Untapped posts heights	—	5.3	—	5.65, 5.38
Posts radii	1	1.5	1.5	1.5
Tapped post distance from sidewall	6, 6	4	6, 6	6, 7.51
Untapped post distance from sidewall	—	8.5	—	3.37, 4.95
Tap point height	1.05, 1.05	0.9	1	1, 0.9
Tapped coupling screw depth	1.84, 1.84	1.43	1.3, 1.3	0.8, 0.62
Untapped coupling screw depth	—	1.75	—	1.63, 1.34
Cavity tuning screw depth	—	—	1.59	—
Waveguide window wall length	—	7	—	7.88

SST: same-sign triplet; OST: opposite-sign triplet.

TABLE 2. Comparison with some related prior-art designs.

Characteristic	[21]	[22]	[30]	This work
Number of resonance modes	2	2	3	3
Synthesized controllable TZs	No	No	No	Yes (at both sides)
Type of inter-mode coupling	Inductive probe (non-tunable)	Capacitive probe (tunable)	Not defined	Coupling screw (fully tunable)
Type of external coupling	Tapped coaxial	Tapped coaxial	Coaxial SMA	Both waveguide and coaxial
Fractional bandwidth	3%	3%	29%	$2\% - 3\%$

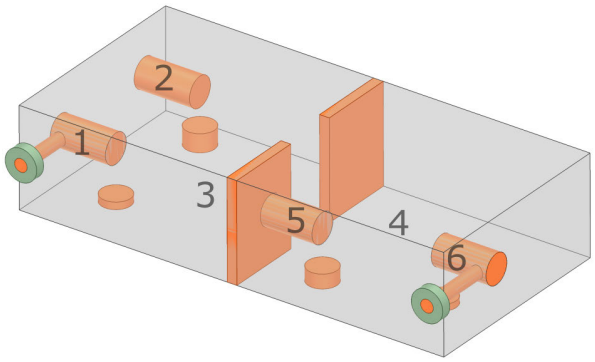

FIGURE 11. Sixth-order filter with a TZ at both passband sides by cascading two triple-mode integrated coaxial-waveguide stages.

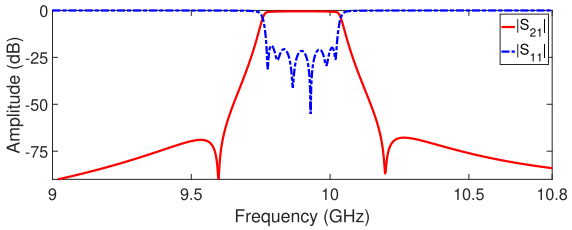

FIGURE 12. EM-simulated power transmission ($|S_{21}|$) and reflection ($|S_{11}|$) responses of the sixth-order filter example corresponding to the 3-D layout shown in Fig. 11.

V. DESIGN EXAMPLE III: HIGHER-ORDER FILTER

In Sections III and IV, the design principle of integrated coaxial-waveguide triplet filters with a TZ below or above the passband has been presented. The purpose here is to extend this concept to realize a sixth-order quasi-elliptic-type bandpass filter with a TZ at both passband sides. To this aim, two filtering stages consisting of same-sign and opposite-sign triplets are inter-cascaded. The prefixed specifications are 9.9-GHz center frequency, bandwidth of 250 MHz—i.e., 2.5% relative bandwidth—, 20-dB minimum in-band input-power-matching level, and lower and upper TZs located at 9.6 GHz and 10.2 GHz, respectively,

The physical 3-D layout of the sixth-order bandpass filter is presented in Fig. 11, whereas the final dimensions of its optimized geometry are listed in Table 1. For the same-sign triplet stage, both posts are placed side-by-side at the end wall. In the opposite-sign triplet stage, one of the posts is positioned at the end wall and the second post is placed at the opposite wall—i.e., the inductive window wall separating the two cavities. For practical reasons, the complete design can either be 3D metal printed or it can be milled in three different parts to be subsequently assembled together, i.e., (i) base, (ii) frame including coupling windows, and (iii) top lid. Furthermore, the post can also be fabricated separately and then fit in the window wall of the filter and heat-treated to solidify the connection to the base unit, as it was done in [35]. Alternatively, posts 5 and 6 could be placed in the sidewalls and move the output coupling SMA connector from the side wall to the end wall to obtain the same filtering response.

From Table 1, it can be verified that the coupling screws realizing weak cross-couplings—i.e., between the tapped posts and the waveguide—have much smaller height when compared to the coupling screws used to implement strong direct couplings—i.e., between the waveguide and the untapped posts. The optimized EM-simulated scattering parameters of this bandpass filter design are represented in Fig. 12, which fairly fulfill the expectations.

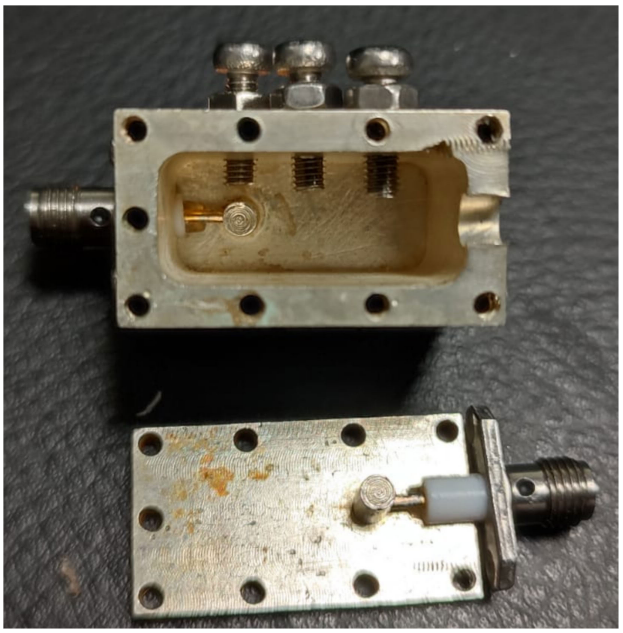

FIGURE 13. Photograph of the manufactured prototype of triplet filter with a TZ below the passband.

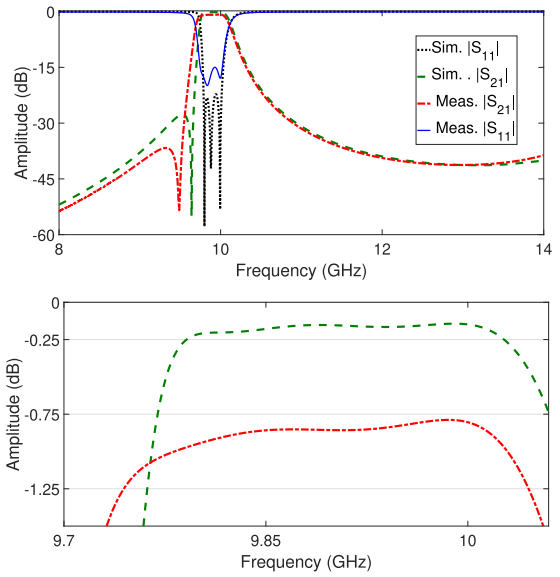

FIGURE 14. EM-simulated and measured power transmission ($|S_{21}|$) and reflection ($|S_{11}|$) responses of the manufactured prototype of triplet filter with a TZ below the passband. (a) Wideband response. (b) In-band detail..

VI. EXPERIMENTAL RESULTS

For practical-validation purposes, one triplet bandpass filter prototype with a TZ located below the passband has been developed and tested. Its photograph is given in Fig. 13. The filter was manufactured in three pieces—main body and two sidewalls—using CNC machining. The coaxial posts were machined directly in the sidewalls. The SMA connectors were soldered directly to the coaxial posts, and then all three parts were assembled together using threaded metal screws to form a closed box. Two coaxial-to-waveguide coupling-tuning screws with 3-mm diameter were placed at the top lid aligned with the post heights. A third cavity-resonance tuning screw was additionally placed right at the center of the cavity at the top lid to allow post-fabrication tuning—so that to compensate manufacturing inaccuracies. The physical dimensions of the final fabricated prototype are summarized in Table 1. Note that it is always required to have minimum additional movable parts to minimize space, volume, and in-band insertion loss in the filter. The fabricated design was just a proof-of-concept prototype aimed at ensuring maximum post-fabrication tuning to counteract possible discrepancies due to manufacturing tolerances. However, the design can be either metal 3D printed in one go or it can be milled in two parts—i.e., base along with frame and top lid—where only a cavity tuning screw may be required and the remaining two coupling screws can be part of the milled cavity frame. This would allow further reducing the space as well as the additional losses in the filter passband due to the screws. Nevertheless, at the same time and as a trade-off, by fixing the coupling screws then the post-fabrication tuning capabilities would be limited.

A comparison between the EM-simulated and measured power transmission and reflection responses of the constructed prototype of integrated coaxial-waveguide-resonator-based bandpass filter is provided in Fig. 14. As can be seen, apart from a small shifting to a lower frequency of the measured response—which is attributed to manufacturing errors in the dimensions of the posts and the outer cavities—, a reasonable agreement between EM-simulated and experimental results is obtained. The main measured characteristics of this prototype are center frequency of 9.878 GHz, bandwidth equal to 259 MHz—i.e., of about 2.6% in relative terms—, minimum in-band insertion-loss level of 0.85 dB, and in-band input-power-matching levels higher than 14.89 dB. It should be remarked upon that in the fabricated prototype, tuning screws were used to tune the resonances and inter-modal couplings. However, there was not any mechanism involved to control the external couplings. It is observed that the design is quite sensitive to the tapping position. Therefore, the difference between the measured and simulated results is mainly associated to it. One possibility to avoid this situation is to use the second resonance of the post. This will require a thicker and longer post and the tapping could be further away from the waveguide wall. In any case, the measured performance fairly attests the experimental viability of the proposed 3-D filter design principle.

Finally, Table 2 shows a comparison of the devised 3-D bandpass filter approach with some related prior-art designs. As can be seen, the filter of this work exploits a higher number of modes for passband shaping, allows to realize TZs with flexible positioning at both passband sides, and offers different variants for the practical implementation of its constituent triple-mode integrated coaxial-waveguide resonator.

VII. CONCLUSION

A design approach to realize compact-size cross-coupled 3-D bandpass filters in inline physical topologies is reported.

It exploits a type of triple-mode integrated coaxial-waveguide resonator as building triplet filtering block. Different implementation variants to flexibly allocate the TZ at either side of the passband depending on the positioning of the posts inside the core rectangular waveguide cavity, as well as multi-stage/higher-order designs, have been illustrated through various EM-simulated 9.9-GHz filter examples. Furthermore, for experimental-demonstration purposes, a proof-of-concept prototype of third-order triplet bandpass filter with a TZ below the passband has been fabricated and characterized.

REFERENCES

[1] M. Yuceer, "A reconfigurable microwave combline filter," *IEEE Trans. Circuits Syst. II, Exp. Briefs*, vol. 63, no. 1, pp. 84–88, Jan. 2016.

[2] J.-X. Xu, M. Huang, H.-Y. Li, Y. Yang, and X. Y. Zhang, "Design of balanced filtering rat-race coupler based on quad-mode dielectric resonator," *IEEE Trans. Circuits Syst. II, Exp. Briefs*, vol. 68, no. 7, pp. 2267–2271, Jul. 2021.

[3] H.-Y. Li, J.-X. Xu, and X. Y. Zhang, "Design of balanced filtering rat-race coupler based on quad-mode dielectric resonator," *IEEE Trans. Circuits Syst. II, Exp. Briefs*, vol. 69, no. 6, pp. 2707–2711, Jun. 2022.

[4] M. A. Chaudhary and M. M. Ahmed, "Pseudoelliptic waveguide filters using U-shaped ridge resonators," *IEEE Trans. Circuits Syst. II, Exp. Briefs*, vol. 70, no. 2, pp. 371–375, Feb. 2023.

[5] M. Latif, G. Macchiarella, and F. Mukhtar, "A novel coupling structure for inline realization of cross-coupled rectangular waveguide filters," *IEEE Access*, vol. 8, pp. 107527–107538, 2020.

[6] U. Jankovic, N. Mohottige, and D. Budimir, "Design of ultra compact pseudo-elliptic inline waveguide bandpass filters using inductive bypass coupling for various specifications," in *Proc. Act. Passive RF Devices*, May 2017, pp. 1–6.

[7] M. Y. Sandhu and I. C. Hunter, "Miniaturized dielectric waveguide filters," *Int. J. Electron.*, vol. 103, no. 10, pp. 1776–1787, Feb. 2016.

[8] J. Ossorio, S. Cogollos, V. Boria, and M. Guglielmi, "Rectangular waveguide quadruplet filter for satellite applications," in *IEEE MTT-S Int. Microw. Symp. Dig.*, Jun. 2019, pp. 1359–1362.

[9] L. Szydlowski, A. Lamecki, and M. Mrozowski, "Coupled-resonator waveguide filter in quadruplet topology with frequency-dependent coupling—A design based on coupling matrix," *IEEE Microw. Wireless Compon. Lett.*, vol. 22, no. 11, pp. 553–555, Nov. 2012.

[10] D. Miek, P. Boe, F. Kamrath, and M. Höft, "Techniques for the generation of multiple additional transmission zeros in H-plane waveguide filters," *Int. J. Microw. Wireless Technol.*, vol. 12, no. 8, pp. 723–732, Oct. 2020.

[11] X. Shang, W. Xia, and M. J. Lancaster, "The design of waveguide filters based on cross-coupled resonators," *Microw. Opt. Technol. Lett.*, vol. 56, no. 1, pp. 3–8, Jan. 2014.

[12] M. Sandhu, M. Mrozowski, A. Lamecki, and R. Gómez-García, "Inline generalized Chebyshev dielectric waveguide filters with nonlinear frequency-variant inverters," in *IEEE MTT-S Int. Microw. Symp. Dig.*, Nov. 2021, pp. 189–191.

[13] M. Mul, A. Lamecki, R. Gómez-García, and M. Mrozowski, "Inverse nonlinear eigenvalue problem framework for the synthesis of coupled-resonator filters with nonresonant nodes and arbitrary frequency-variant reactive couplings," *IEEE Trans. Microw. Theory Techn.*, vol. 69, no. 12, pp. 5203–5216, Dec. 2021.

[14] D. Miek, A. Morán-López, J. A. Ruiz-Cruz, and M. Höft, "Ku-band waveguide filter with multiple transmission zeros by resonant source to load and bypass cross-coupling," in *Proc. 49th Eur. Microw. Conf. (EuMC)*, Oct. 2019, pp. 57–60.

[15] Y. Wang and M. Yu, "True inline cross-coupled coaxial cavity filters," *IEEE Trans. Microw. Theory Techn.*, vol. 57, no. 12, pp. 2958–2965, Dec. 2009.

[16] R. Tkadlec and G. Macchiarella, "Pseudoelliptic combline filter in a circularly shaped tube," in *IEEE MTT-S Int. Microw. Symp. Dig.*, Jun. 2018, pp. 1099–1102.

[17] M. Hoft and F. Yousif, "Orthogonal coaxial cavity filters with distributed cross-coupling," *IEEE Microw. Wireless Compon. Lett.*, vol. 21, no. 10, pp. 519–521, Oct. 2011.

[18] S. Bastioli, R. V. Snyder, and G. Macchiarella, "Design of in-line filters with strongly coupled resonator triplet," *IEEE Trans. Microw. Theory Techn.*, vol. 66, no. 12, pp. 5585–5592, Dec. 2018.

[19] G. Macchiarella, S. Bastioli, and R. V. Snyder, "Design of in-line filters with transmission zeros using strongly coupled resonators pairs," *IEEE Trans. Microw. Theory Techn.*, vol. 66, no. 8, pp. 3836–3846, Aug. 2018.

[20] J. J. Vague, D. Rubio, M. A. Fuentes, S. Cogollos, M. Baquero, V. E. Boria, and M. Guglielmi, "Inline combline filters of order N with up to $N+1$ transmission zeros," *IEEE Trans. Microw. Theory Techn.*, vol. 69, no. 7, pp. 3287–3297, Jul. 2021.

[21] A. A. San-Blas, J. C. Melgarejo, V. E. Boria, and M. Guglielmi, "Novel solution for the coaxial excitation of inductive rectangular waveguide filters," in *Proc. 48th Eur. Microw. Conf. (EuMC)*, Sep. 2018, pp. 89–92.

[22] Á. A. San-Blas, M. Guglielmi, J. C. Melgarejo, Á. Coves, and V. E. Boria, "Design procedure for bandpass filters based on integrated coaxial and rectangular waveguide resonators," *IEEE Trans. Microw. Theory Techn.*, vol. 68, no. 10, pp. 4390–4404, Oct. 2020.

[23] M. S. Bakr, "Triple-mode microwave filters with arbitrary prescribed transmission zeros," *IEEE Access*, vol. 9, pp. 22045–22052, 2021.

[24] M. S. Bakr, I. C. Hunter, and W. Bösch, "Miniature triple-mode dielectric resonator filters," *IEEE Trans. Microw. Theory Techn.*, vol. 66, no. 12, pp. 5625–5631, Dec. 2018.

[25] A. Panariello and M. Guglielmi, "Triple-mode asymmetric filters in a rectangular waveguide," *Microw. Opt. Technol. Lett.*, vol. 28, no. 4, pp. 228–231, Feb. 2001.

[26] H. Salehi, T. Bernhardt, T. Lukkarila, and S. Amir, "Analysis, design and applications of the triple-mode conductor-loaded cavity filter," *IET Microw., Antennas, Propag.*, vol. 5, pp. 1136–1142, Jul. 2011.

[27] S. Amari and U. Rosenberg, "A circular triple-mode cavity filter with two independently controlled transmission zeros," in *Proc. Eur. Microw. Conf.*, Sep. 2006, pp. 1091–1094.

[28] S. Bastioli and R. V. Snyder, "New triple-resonance configuration using stubbed waveguide dual-mode cavities," *IEEE Microw. Wireless Compon. Lett.*, vol. 32, no. 6, pp. 652–655, Jun. 2022.

[29] S.-W. Wong, Z.-C. Guo, J.-Y. Lin, L. Zhu, and Q. Zhang, "Triple-mode and triple-band cavity bandpass filter on triplet topology with controllable transmission zeros," *IEEE Access*, vol. 6, pp. 29452–29459, 2018.

[30] S.-F. Feng, S.-W. Wong, F. Deng, L. Zhu, and Q.-X. Chu, "Triple-mode wideband bandpass filter using single rectangular waveguide cavity," in *Proc. IEEE Int. Conf. Comput. Electromagn. (ICCEM)*, Feb. 2016, pp. 287–289.

[31] S.-F. Feng, S.-W. Wong, L. Zhu, and Q.-X. Chu, "A triple-mode wideband bandpass filter using single rectangular waveguide cavity," *IEEE Microw. Wireless Compon. Lett.*, vol. 27, no. 2, pp. 117–119, Feb. 2017.

[32] R. Cameron, C. Kudsia, and R. Mansour, *Microwave Filters for Communication Systems*. New York, NY, USA: Wiley, 2007.

[33] L. Balewski, G. Fotyga, M. Mrozowski, M. Mul, P. Sypek, D. Szypulski, and A. Lamecki, "Step on it bringing fullwave finite-element microwave filter design up to speed," *IEEE Microw. Mag.*, vol. 21, no. 3, pp. 34–49, Mar. 2020.

[34] InventSim. (2023). *EM Invent*. [Online]. Available: http://inventsim.com/

[35] M. Y. Sandhu, M. Jasinski, A. Lamecki, R. Gómez-García, and M. Mrozowski, "Inline waveguide filter with transmission zeros using a modified-T-shaped-post coupling inverter," *IEEE Microw. Wireless Technol. Lett.*, vol. 33, no. 2, pp. 145–148, Feb. 2023.

MUHAMMAD YAMEEN SANDHU (Senior Member, IEEE) received the M.Sc. and Ph.D. degrees in electronic and electrical engineering from the University of Leeds, Leeds, U.K., in 2011 and 2014, respectively. In 2009, he joined the Department of Electrical Engineering, Sukkur IBA University, where he is currently an Associate Professor. From 2014 to 2016, he was a Research Fellow with the University of Leeds. From 2021 to 2022, he was a Postdoctoral Research Fellow with the Department of Microwave and Antenna Engineering, Gdańsk University of Technology, Poland. His research interests include microwave filters, microwave sensors, antenna design, and microwave materials processing.

SHARJEEL AFRIDI (Senior Member, IEEE) received the Bachelor of Engineering degree from Mehran UET, Jamshoro, Pakistan, in 2007, and the M.Sc. and Ph.D. degrees from the University of Leeds, U.K., in 2012 and 2018, respectively. He was a Research Associate with the Institute of Information and Communication, University of Sindh, from October 2007 to July 2009. He has been an Associate Professor with the Department of Electrical Engineering, Sukkur IBA University, since July 2009. His research interests include mobile communication systems and microwave filters and measurements.

ADAM LAMECKI (Senior Member, IEEE) received the M.S.E.E. and Ph.D. degrees in microwave engineering from the Gdańsk University of Technology (GUT), Gdańsk, Poland, in 2002 and 2007, respectively. In 2007, he cofounded EM Invent, Gdańsk, a spin-off company, which develops an electromagnetic field simulator InventSim, where he has served as the Chief Technology Officer (CTO). Since 2019, he has been an Associate Professor with the Department of Microwave and Antenna Engineering, GUT. His research interests include filter design and optimization techniques, surrogate models and their application to the computer-aided design (CAD) of microwave devices, and computational electromagnetics (mainly focused on the finite-element method).

ROBERTO GÓMEZ-GARCÍA (Fellow, IEEE) is currently a Full Professor with the Department of Signal Theory and Communications, University of Alcalá, Alcalá de Henares, Spain. His current research interests include the design of fixed/tunable high-frequency filters and multiplexers in planar, hybrid, and monolithic microwave-integrated circuit technologies, multifunction circuits and systems, software-defined radio and radar architectures for telecommunications, remote sensing, and biomedical applications, and displacement RF sensors. In these topics, he has authored/coauthored about 135 articles in international journals and 170 papers in international conferences.

He serves as a member of the technical review board for several IEEE and EuMA conferences. He is also a member of the IEEE MTT-S Filters (MTT-5) Technical Committee, the IEEE MTT-S RF MEMS and Microwave Acoustics (MTT-6) Technical Committee, the IEEE MTT-S Wireless Communications (MTT-23) Technical Committee, the IEEE MTT-S Biological Effects and Medical Applications of RF and Microwave (MTT-28) Technical Committee, and the IEEE CAS-S Analog Signal Processing Technical Committee. He was a recipient of the 2016 IEEE Microwave Theory and Techniques Society (MTT-S) Outstanding Young Engineer Award. He was an Associate Editor of IEEE TRANSACTIONS ON MICROWAVE THEORY AND TECHNIQUES, from 2012 to 2016, IEEE TRANSACTIONS ON CIRCUITS AND SYSTEMS—I: REGULAR PAPERS, from 2012 to 2015, IEEE MICROWAVE AND WIRELESS COMPONENTS LETTERS, from 2018 to 2020, as well as other journals such as IEEE ACCESS, *IET Microwaves, Antennas, and Propagation*, and the *International Journal of Microwave and Wireless Technologies*. He was a Senior Editor of the IEEE JOURNAL ON EMERGING AND SELECTED TOPICS IN CIRCUITS AND SYSTEMS, from 2016 to 2017, and the MTT-S Newsletter Working Group Chair, from 2019 to 2021. He was the guest editor of several special/focus issues and sections in IEEE and IET journals. He is also the Editor-in-Chief of the IEEE MICROWAVE AND WIRELESS TECHNOLOGY LETTERS, an Associate Editor of the IEEE JOURNAL OF ELECTROMAGNETICS, RF AND MICROWAVES IN MEDICINE AND BIOLOGY, the TC-5 Topic Editor of the IEEE JOURNAL OF MICROWAVES, and an Editorial Board Member of *Electromagnetic Science*. He was an IEEE CAS-S Distinguished Lecturer (2020–2022).

MICHAL MROZOWSKI (Fellow, IEEE) received the M.Sc. degree (Hons.) in telecommunication engineering and the Ph.D. degree (Hons.) in electronic engineering from the Gdańsk University of Technology, in 1983 and 1990, respectively.

In 1986, he joined the Department of Electronics, Gdańsk University of Technology, where he is currently a Full Professor, the Head of the Department of Microwave and Antenna Engineering, and the Director of the Doctoral School. He has developed several software modules that have been then integrated into commercial microwave EDA software used all over the world. He has published one book and over 100 peer-reviewed articles in IEEE journals. His research interests include computational electromagnetics, photonics, and microwave engineering. His current work is focused on the development of new fast numerical techniques for solving 2D and 3D boundary value problems in the time and frequency domains, automated microwave filter design, microwave filter synthesis, microwave sensor design, microwave EDA, reduced-order models for grid-based numerical techniques (e.g., FDTD and FEM), and surrogate model construction.

Prof. Mrozowski also serves as a member of the Editorial Board for IEEE ACCESS. He is a member of the MTT-1 and MTT-2 Technical Committees, a fellow of the Electromagnetics Academy, and a member of the Polish Academy of Sciences. Furthermore, he is the past Vice-Dean for Research of the ETI Faculty, and the past Chairperson of the Polish AES/AP/MTT Chapter. He served as an Associate Editor for IEEE MICROWAVE AND WIRELESS COMPONENTS LETTERS and a member of the Editorial Board for the PROCEEDINGS OF THE IEEE.